J. Opt. **13** (2011) 115503 (6pp) doi:10.1088/2040-8978/13/11/115503

Liquid lens with double tunable surfaces for large power tunability and improved optical performance

Lei Li, Qiong-Hua Wang and Wei Jiang

School of Electronics and Information Engineering, Sichuan University, Chengdu 610065, People's Republic of China
and
State Key Laboratory of Fundamental Science on Synthetic Vision, Sichuan University, Chengdu 610065, People's Republic of China

E-mail: qhwang@scu.edu.cn

Received 9 August 2011, accepted for publication 6 October 2011
Published 28 October 2011
Online at stacks.iop.org/JOpt/13/115503

Abstract
In this paper we propose a liquid lens with two tunable interfaces formed by two kinds of immiscible liquids. The proposed liquid lens uses liquid pressure to change the shape of the interfaces. It can provide a large tunable range of optical power and improved optical performance. By applying suitable liquids the gravity effect can also be negligible. To prove the principles, a liquid lens with 7 mm aperture was fabricated. The optical performance indicates that the proposed liquid lens can provide a large tunable range of both positive and negative powers even using liquids with small differences in refractive indices. The resolution is better than 50 lp mm^{-1} under white light environment. The spherical aberration and coma are also largely reduced. The proposed liquid lens can also provide the optical designer with the freedom to choose the combination of liquids to reduce or even correct aberrations.

Keywords: liquid lens, aberration

S Online supplementary data available from stacks.iop.org/JOpt/13/115503/mmedia

(Some figures may appear in colour only in the online journal)

1. Introduction

In recent years, researchers have shown great interest in liquid lenses for its potential applications such as image processing, zoom lenses, 3D displays, portable electronic devices and so on [1–9]. The liquid lens is also attractive for its easy fabrication, compact structure and low cost. Several types of liquid lenses have been proposed and the technology is also in progress.

A membrane liquid lens [1–4] is a typical fluidic pressure-based lens. The elastic membrane is sealed in the aperture. By applying a pressure, the shape of the deformable surface is changed which results in the focal length tuning. The PDMS membrane is often used in this type of lens. The membrane liquid lens has many advantages such as large lens aperture, compact structure and easy operation. The tuning range of the focal length is also very large. However, the gravity effect is a great problem in this type of lens when it is placed in a vertical position.

Electro-wetting lenses and dielectric lenses [5–9] are also commonly used liquid lenses. Both the electro-wetting lens and dielectric lens use an external voltage to change the focal length. For the electro-wetting lens, a conducting liquid drop forms a contact angle on a solid surface, and it is surrounded by another immiscible insulating fluid. For the dielectric lens, the two liquids employed in the dielectric lens are nonconductive but with different dielectric constants and they exhibit a very smooth liquid–liquid interface. If the liquids match in density, the gravity effect can be negligible. Recently, another type of liquid lens, called an adaptive mechanical-wetting lens, has been demonstrated [10]. It uses mechanical force to change the shape of the liquid–liquid interface rather than external voltage. These types of lenses can minimize the gravity effect and obtain a smooth liquid–liquid interface. However, for

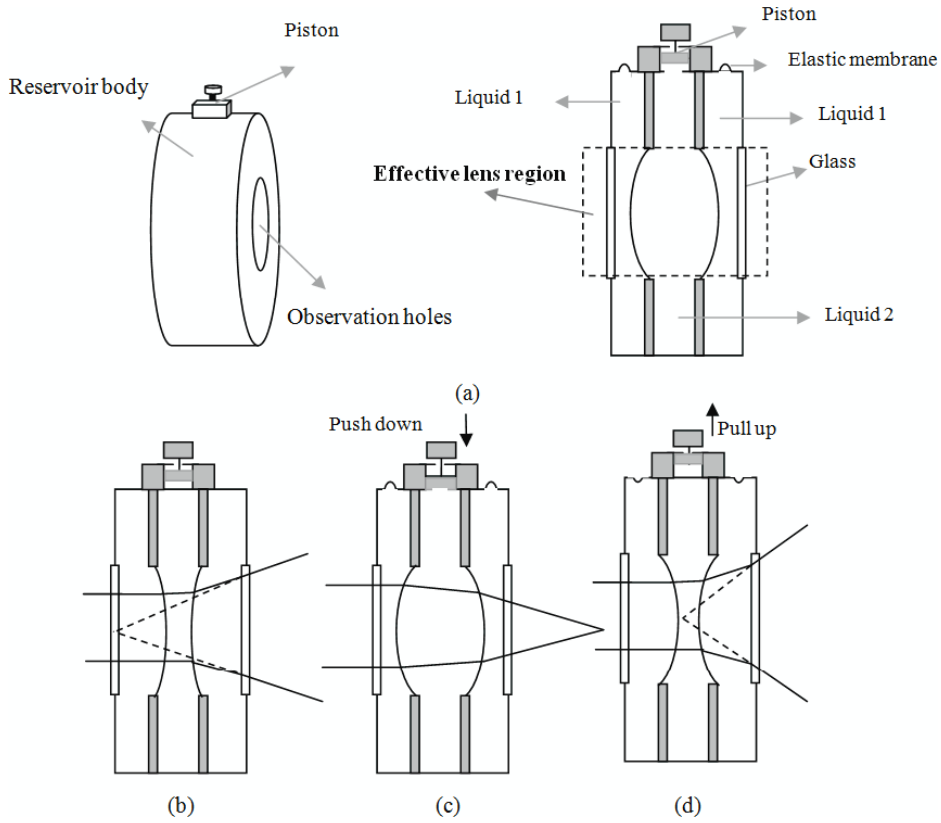

Figure 1. The structure of proposed liquid lens. (a) The whole device and side view of the device. (b) Initial state. (c) Further positive state. (d) Further negative state.

these types of lenses the tuning range of the focal length is determined by the refractive index difference. Usually, the refractive index difference is very small due to the limited available liquids. So the tuning range of focal length is not large. Besides, due to the plano-convex surface, the optical performance is poor, with small f number.

In this paper, we propose an adaptive liquid lens. It retains the advantages of the electro-wetting lens and mechanical-wetting lens such as smooth interface and minimum gravity effect. However, the proposed liquid lens can provide about two times larger tuning ability of optical power and the optical performance is greatly improved. The proposed liquid lens also provides the designer with the freedom to choose liquids to balance the aberrations to meet the optical requirements.

2. Device structure and theoretical analysis

The structure of the proposed liquid lens is shown in figure 1. It consists of three main parts including piston, reservoir body and observation holes as shown in figure 1(a). From the side view, we see that the effective lens region is in the center of the reservoir body with two observation holes covered by glass. There are also two holes near the piston covered by an elastic membrane. In the main body there are three sub-chambers filled with two immiscible liquids (one liquid filled in the center chamber and the other liquid filled in the side chambers). Therefore, they form two liquid–liquid interfaces. Figure 1(b) is the initial state. When the piston is pushed down, the center liquid will press the side liquid to form bending in the interfaces. At this time, the surplus liquid in the side chamber will flow into the space formed by the elastic membrane. When the piston is pulled up, the side liquid will press the center liquid to form bending in the interfaces as shown in figures 1(c) and (d).

2.1. Analysis of the optical power of the proposed liquid lens

Figure 2 is the view of the effective lens region. We treat the interfaces as a spherical profile for the following analysis [5–7]. The optical power of the liquid lens can be calculated as follows:

$$\phi = (n_2 - n_1)(c_1 - c_2) + \frac{(n_2 - n_1)^2 d_2}{n_2} c_1 c_2, \qquad (1)$$

where c_1 and c_2 are the curvatures of the interfaces. d_2 is the thickness between the interfaces. and n_1 and n_2 are the refractive indices. Because the structure of the proposed liquid lens is symmetrical, the curvature c_1 is equal to $-c_2$ when the liquid lens is used in the vertical position. Equation (1) can be rewritten:

$$\phi = 2(n_2 - n_1)c_1 - \frac{(n_2 - n_1)^2 d_2}{n_2} c_1^2. \qquad (2)$$

Thus it can provide a power about two times larger than the traditional electro-wetting lens or adaptive mechanical-wetting lens (with power $(n_2 - n_1)c$, where c is the curvature of the interface).

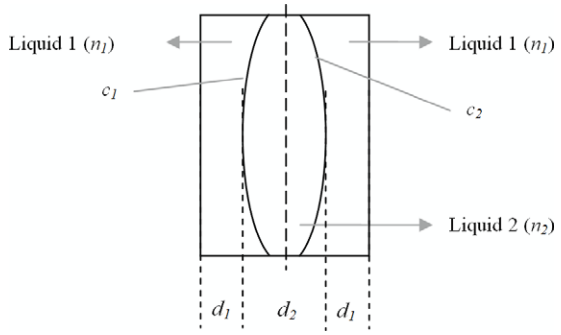

Figure 2. View of effective lens region.

2.2. Analysis of monochromatic aberrations of the proposed liquid lens

As shown in figure 2, the proposed liquid lens can be viewed as two double liquid lenses in contact (separated by the virtual vertical line in the center). According to third-order theory [11], using the thin lens approximation after some mathematical manipulation, the spherical aberration coefficient of third order for the one interface with the two liquid lenses (electro-wetting lens or mechanical-wetting lens) can be obtained as follows when the object is at infinity [12]:

$$S_{\mathrm{I}} = h^4 A \phi^3, \tag{3}$$

$$A = 1 + \frac{2n_1 - n_2}{n_2(n_2 - n_1)^2}, \tag{4}$$

where h is the height of the marginal ray. c is the curvature of the interface. n_1 and n_2 represent the refractive indices of the liquids in the front and back chambers, respectively.

We assume that the spherical aberration coefficient of the 'first lens' (the part on the left of the virtual vertical line in the center in figure 2) is S_{I1} and that of the 'second lens' (the part on the right of the virtual vertical line in the center in figure 2) is S_{I2}. We can obtain the spherical aberration coefficient of third order for the proposed liquid lens as follows when the object is at infinity:

$$\sum S_{\mathrm{I}} = S_{\mathrm{I1}} + S_{\mathrm{I2}}. \tag{5}$$

By substituting equations (3) and (4) into (5), we can get

$$\sum S_{\mathrm{I}} = h^4(A_1\phi_1^3 + A_2\phi_2^3), \tag{6}$$

where ϕ_1 is the power of the 'first lens' and ϕ_2 is the power of the 'second lens'. Because the curvature c_1 is equal to $-c_2$, the power ϕ_1 is equal to ϕ_2. Thus we can get

$$\phi_1 = \phi_2 = \frac{\phi}{2}. \tag{7}$$

By substituting equations (7) into (6), we get

$$\sum S_{\mathrm{I}} = \tfrac{1}{8}h^4(A_1 + A_2)\phi^3. \tag{8}$$

$$A_1 = 1 + \frac{2n_1 - n_2}{n_2(n_2 - n_1)^2}, \tag{9}$$

$$A_2 = 1 + \frac{2n_2 - n_1}{n_1(n_2 - n_1)^2}, \tag{10}$$

where ϕ is the power of the proposed lens.

Similar derivations can be made for other monochromatic aberrations when the object is at infinity as follows:

$$\sum S_{\mathrm{II}} = \tfrac{1}{8}\bar{h}h^3(A_1 + A_2)\phi^3 - \tfrac{1}{4}Hh^2(B_1 + B_2)\phi^2, \tag{11}$$

$$\sum S_{\mathrm{III}} = \tfrac{1}{8}\bar{h}^2h^2(A_1 + A_2)\phi^3 - \tfrac{1}{2}H\bar{h}h \times (B_1 + B_2)\phi^2 + H^2\phi, \tag{12}$$

$$\sum S_{\mathrm{IV}} = C\phi, \tag{13}$$

$$\sum S_{\mathrm{V}} = \tfrac{1}{8}\bar{h}^3h(A_1 + A_2)\phi^3 - \tfrac{3}{4}H\bar{h}^2(B_1 + B_2)\phi^2 + H^2(\bar{h}/h)(3 + C)\phi, \tag{14}$$

$$B_1 = 1 + \frac{1}{n_2(n_1 - n_2)}, \tag{15}$$

$$B_2 = 1 + \frac{1}{n_1(n_2 - n_1)}, \tag{16}$$

$$C = \frac{1}{n_1 n_2}, \tag{17}$$

where $\sum S_{\mathrm{II}}$, $\sum S_{\mathrm{III}}$, $\sum S_{\mathrm{IV}}$ and $\sum S_{\mathrm{V}}$ are coma, astigmatism, field curvature and distortion coefficient of third order for the proposed liquid lens, respectively. $\bar{h}$ is the incident height of the paraxial chief ray and H is the Lagrange–Helmholtz invariant.

For the proposed liquid lens, the power is distributed equally to the two curvatures c_1 and c_2. Therefore, the bending of the proposed liquid lens is much smaller than that of the conventional liquid lens (electro-wetting lens or mechanical-wetting lens), which results in reduced aberrations. We assume the refractive indices of the liquids (n_1 and n_2) vary from 1.3 to 1.8. For spherical aberration (equation (8)), the factor $A_1 + A_2$ is larger than A_1 (the factor of the electro-wetting lens or mechanical-wetting lens). The maximum of $|(A_1 + A_2)/A_1|$ is 2.96 (this result is gotten based on mathematic calculation). However, the other factor is reduced to 1/8 because of the reduced bending. So the spherical aberration of the proposed liquid lens is greatly reduced compared to that of the conventional liquid lens. For the coma (equation (11)), the factor $B_1 + B_2$ is no larger than B_1. The maximum of $|(B_1 + B_2)/B_1|$ is 1.603. Therefore, the coma aberration of the proposed liquid lens is also greatly reduced. For astigmatism (equation (12)), if the factor $\frac{1}{8}\bar{h}^2h^2(A_1 + A_2)\phi^3 - \frac{1}{2}H\bar{h}h(B_1 + B_2)\phi^2$ makes the largest contribution to the whole astigmatism, the astigmatism of the proposed liquid lens is also greatly reduced. For field curvature (equation (13)), there is no difference between the proposed liquid lens and the conventional one. For distortion (equation (14)), if the factor $\frac{1}{8}\bar{h}^3h(A_1 + A_2)\phi^3 - \frac{3}{4}H\bar{h}^2(B_1 + B_2)\phi^2$ make the largest contribution to the whole distortion, the distortion of the proposed liquid lens is also greatly reduced.

We can see from equations (12)–(17) that, although it is uncertain whether the astigmatism and distortion is to be reduced, we can also choose the combination of liquids (n_1 and n_2), which determines the value of the factor $A_1 + A_2$ and $B_1 + B_2$, to reduce the aberrations, except field curvature. to meet the optical requirement.

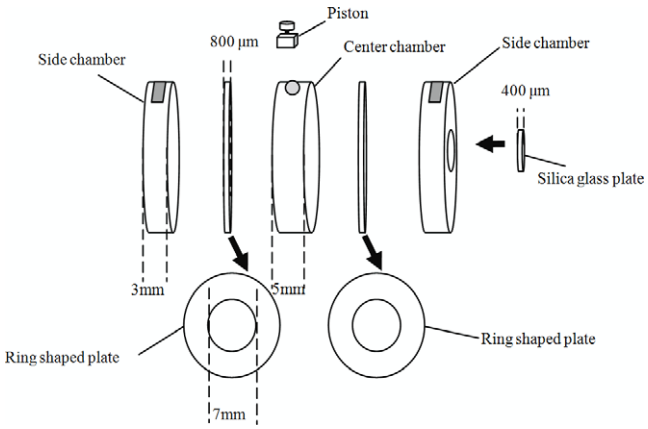

Figure 3. Fabrication of the proposed liquid lens.

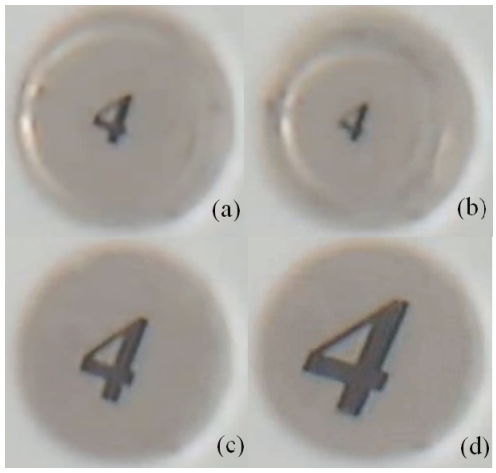

Figure 4. Images for different focal lengths (Media 1 available at stacks.iop.org/JOpt/13/115503/mmedia). (a) State 1. (b) State 2. (c) State 3. (d) State 4.

3. Experiment and result discussion

Figure 3 shows the fabrication of the proposed liquid lens. The three chambers of the reservoir body were made of PMMA (polymethylmethacrylate). The ring-shaped plates with a hole in the center connect the three chambers to form the main body. The ring-shaped plates were made of transparent plastic slabs with 7 mm aperture in the center. In the side chambers, there are two rectangular-shaped holes sealed with PDMS (polydimethylsiloxane). In the center chamber, there is a circular-shaped hole into which the piston is put. We also introduce a 400 μm thin silica glass plate sealed in the side chambers as a observation hole. The thickness of the side chamber is about 3 mm. The thickness of the center chamber is about 5 mm as shown in figure 3. The whole length of the device is less than 14 mm. The liquid filled in the side chambers is a solution of 20% lithium chloride (a refractive index of 1.38, a density of 1.115 g cm^{-3}), while the liquid filled in the center chamber is OPTICAL GEL CODE 081160 [13] (a refractive index of 1.52, a density of 1.110 g cm^{-3}).

We put a printed number '4' very near to the lens; thus the object distance is always within the focal length of the lens. Therefore, we can observe an upright virtual image. In the experiment. We put a CCD camera behind the lens to record the image during the transition process. Figure 4 shows the images taken through the lens for different focusing states. The first state is shown in figure 4(a). When we pulled up the piston, the liquid in the center became less. Therefore the interfaces became concave to the center liquid corresponding to the state in figure 1(d). The lens had negative focal length so the image was reduced as shown in figure 4(b). When we pushed down the piston, the liquid in the center became more. The interfaces became convex. The lens had positive focal length, so the image was magnified as shown in figure 4(c). When we further pushed down the piston corresponding to the state in figure 1(c), the image was further magnified as shown in figure 4(d).

We also calculated the focal lengths of the four states (in figure 4) as shown in table 1. From the table, we can see that the shortest focal lengths are −12.6 mm for the negative state and 12.5 mm for the positive state, respectively. The tuning range is very large as a liquid lens. We can see that the focal length is relatively large in State 3. The image size in State 3 is very close to the size of the object. So State 3 is almost a non-focusing state.

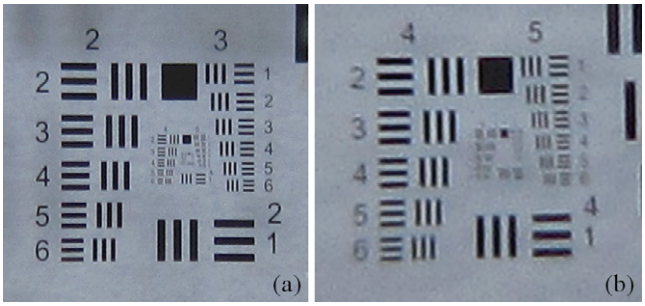

Figure 5. Lens resolution. (a) Initial state. (b) Focusing state.

Table 1. Optical parameters of four states.

	State 1	State 2	State 3	State 4
Focal length (mm)	−15.1	−12.6	140.0	12.5

Figure 5 shows the image of a 1951 US Air Force (USAF) resolution target taken under white light environment. Figure 5(a) shows the image taken in the initial state. Figure 5(b) shows the image taken in the focusing state. We can see that group 5 number 5 is still resolvable. The highest resolution of the device is about 50 lp mm^{-1}.

To evaluate the optical performance, we modeled the proposed liquid lens in Zemax-EE. As a comparison, we also modeled an electro-wetting lens (or mechanical-wetting lens) with the same liquids (a refractive index of 1.38 and a refractive index of 1.52). The object is at infinity and the field angle is 20°. The simulation result of monochromatic aberrations as a function of focal length is shown in figure 6. Before the focal length of 26 mm, only the aberrations of the proposed liquid lens appear in the map. That is because only the proposed liquid lens can provide such a short focal length with the

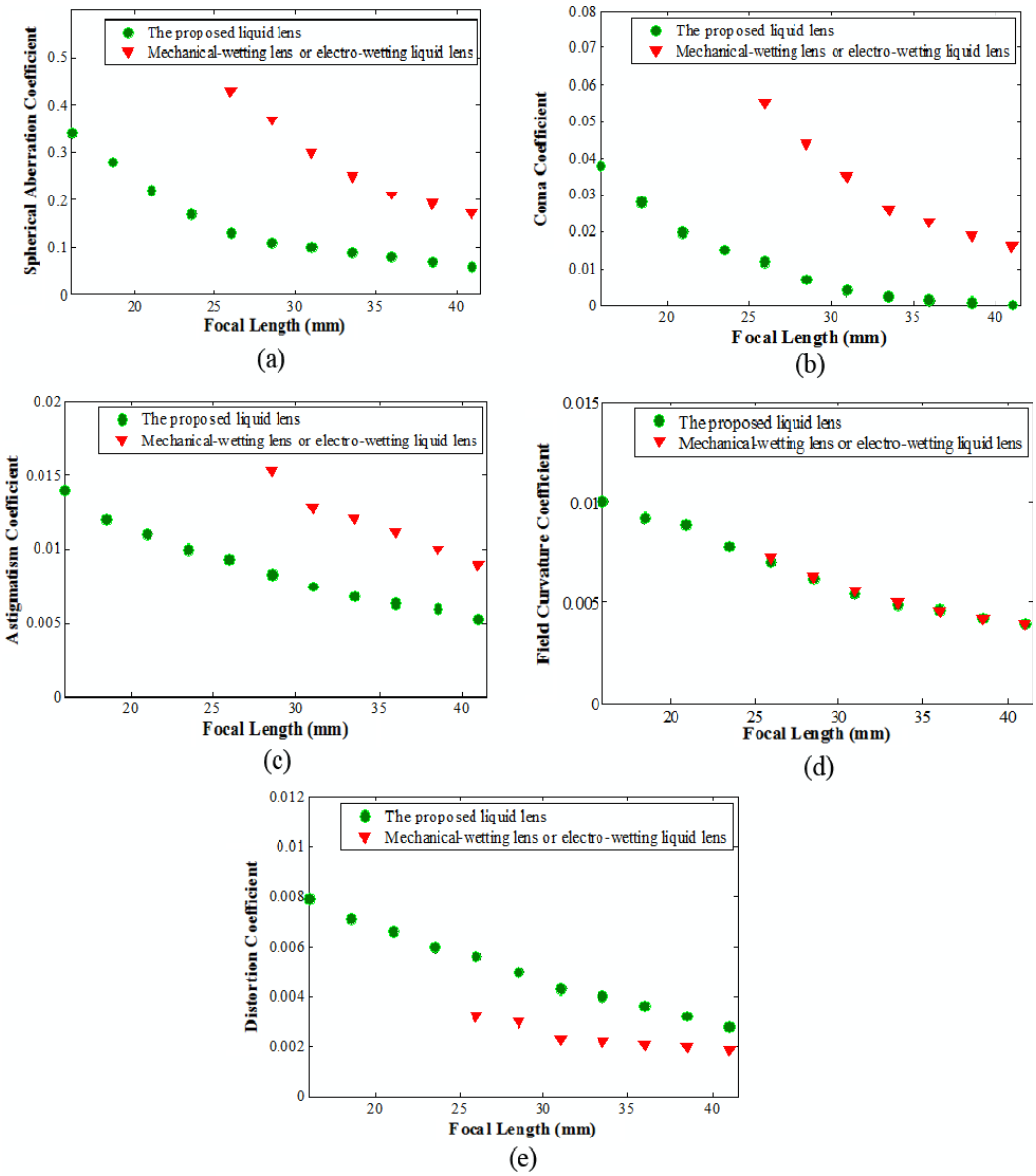

Figure 6. Monochromatic aberration coefficient of the proposed liquid lens and electro-wetting lens or mechanical-wetting lens. (a) Spherical aberration. (b) Coma. (c) Astigmatism. (d) Field curvature. (e) Distortion.

small refractive index difference of the two liquids (a refractive index of 1.38 and a refractive index of 1.52). Comparing the aberrations with the same focal length, we can see that the spherical aberration and coma of the proposed liquid lens are greatly reduced as shown in figures 6(a) and (b). The astigmatism is also reduced as shown in figure 6(c). Also the field curvature remains the same as that of the electro-wetting lens (or mechanical-wetting lens) as shown in figure 6(d). However, distortion is a little worse as shown in figure 6(e). On the whole, the optical performance of the proposed liquid lens is improved. We note that although the simulation result of distortion of the proposed liquid lens is worse than that of the electro-wetting lens (or mechanical-wetting lens), the proposed liquid lens can also obtain better results by choosing the correct liquids. Therefore, an optical designer can try combinations of different liquids to meet the design requirement.

We compare the experimental data with the theoretical calculation result. Table 2 gives a comparison of the shortest focal lengths between measurements and calculations based on equation (2). There is a little difference between experiments and the calculations. The difference may result from the experimental error. Table 3 gives a comparison of spherical aberration coefficients between ray tracing results and the calculations based on equations (8)–(10). We can see that, when the focal length is larger, the agreement is better. The difference may result from an approximation of thin lens structure in the calculations. On the whole, the calculations agree with the experimental data. Therefore, the derived calculations in section 2 on optical characteristics can be used for estimating optical characteristics of the proposed liquid lens.

We also note that, as for our fabricated liquid lens, the interface is not perfectly spherical because the liquids'

Table 2. Comparison of focal lengths between the experiment and theoretical calculation.

	The shortest negative focal length (mm)	The shortest positive focal length (mm)
Experiment	−12.6	12.5
Calculation	−13.1	13.9

Table 3. Comparison of spherical aberration coefficient between the ray trace result and theoretical calculation.

Focal length	18 mm	20 mm	22 mm	24 mm	26 mm	28 mm	30 mm
Ray trace result	0.291	0.271	0.216	0.167	0.122	0.109	0.100
Calculation	0.336	0.256	0.193	0.148	0.114	0.095	0.087

densities are not fully matching (the difference of the two fluids' densities is 0.005 g cm^{-3}). The liquid interface tends to deform with a coma shape [14]. Therefore, the proposed liquid lens also suffers from a coma aberration due to the mismatch in densities. The coma aberration in WFE (wave front error) of the fabricated liquid lens is about 377 nm. It also suffers from an additional 493 nm of WFE every 10 °C due to the expansion coefficient mismatch. The calculations are described in detail in [14]. Besides, sphericity of the ring-shaped plates also affect the performance of astigmatism and coma. Therefore, to get the best performance of the proposed liquid lens, the fabrication technique still needs to be improved and the densities of liquids should be well matched, especially for a large aperture liquid lens. If it is used for an outdoor application, liquid densities should be well matched over a certain temperature range.

From the experiments, we see that the proposed liquid lens performs very well. The proposed liquid lens can provide a large tuning range of focal length with improved optical performance. Lens designers often find it is very difficult to find immiscible liquids matched in density with large refractive index difference, because the liquids can be used is very limited. The proposed liquid lens help to ease the problem. Even using liquids with small refractive index difference, for example the liquids used in the experiment (1.38 and 1.52), the proposed liquid lens can also provide a large tuning range of focal length. Besides, since the proposed liquid lens employs no PDMS, it can extend their working range to the infrared region by choosing the proper liquids. If we can find the proper three immiscible liquids matched in density, the chromatic aberration can also be corrected by the proper combination of the liquids. Besides, if a mechanical motor is used, the proposed lens can achieve automatic driving and fast response. We also note that, since the proposed liquid lens system uses a sandwich shape of two liquids, the liquid lens is not suitable to be used in a situation with violent shaking or vibrating. We believe that, with the development of liquid lenses (such as more liquids available, mechanical motor available and so on), the proposed liquid lens can extend its potential functions.

4. Conclusion

We propose a liquid lens with two tunable interfaces formed by two kinds of immiscible liquids. The proposed liquid lens uses the liquid pressure to change the shape of the interfaces. It can provide a large tunable range of optical power and the spherical aberration is also reduced. By applying suitable liquids the gravity effect can also be negligible. A liquid lens with 7 mm aperture was fabricated. The optical performance indicates that the proposed liquid lens can provide a large tunable range of power even using liquids with small differences in refractive index. The spherical aberration and coma are also greatly reduced. The proposed liquid lens can also provide the optical designer with the freedom to choose the combination of liquids to reduce or even correct the aberrations. It also has potential functions with the development of liquid lenses.

Acknowledgments

The work is supported by the National Natural Science Foundation of China under grant nos. 60877004 and 61036008. The authors would like to thank Xiao-Qing Xu and Jun Liu for their technical assistance.

References

[1] Ren H and Wu S T 2007 Variable-focus liquid lens *Opt. Express* **15** 5931–6
[2] Lee S W and Lee S S 2007 Focal tunable liquid lens integrated with an electromagnetic actuator *Appl. Phys. Lett.* **90** 121129
[3] Ren H, Fox D, Anderson P A, Wu B and Wu S T 2006 Tunable-focus liquid lens controlled using a servo motor *Opt. Express* **14** 8031–6
[4] Zhang D Y, Lien V, Berdichevsky Y, Choi J and Lo Y H 2003 Fluidic adaptive lens with high focal length tunability *Appl. Phys. Lett.* **82** 3171–2
[5] Kuiper S and Hendriks B H W 2004 Variable-focus liquid lens for miniature cameras *Appl. Phys. Lett.* **85** 1128–30
[6] Berge B and Peseux J 2000 Variable focal lens controlled by an external voltage *Eur. Phys. J.* E **3** 159–63
[7] Sugiura N and Morita S 1993 Variable-focus liquid-filled optics lens *Appl. Opt.* **32** 4181–6
[8] Hendriks B H W, Kuiper S, Van As M A J, Renders C A and Tukker T W 2005 Electrowetting-based variable-focus lens for miniature system *Opt. Rev.* **12** 255–9
[9] Ren H, Xianyu H, Xu S and Wu S T 2008 Adaptive dielectric liquid lens *Opt. Express* **16** 14954–60
[10] Xu S, Liu Y, Ren H and Wu S T 2010 A novel adaptive mechanical-wetting lens for visible and near infrared imaging *Opt. Express* **18** 12430–5
[11] Welford W T 1974 *Aberrations of the Symmetrical Optical System* (New York: Academic)
[12] Miks A and Novak J 2010 Third-order aberrations of the thin refractive tunable-focus lens *Opt. Lett.* **35** 1031–3
[13] Cargille Laboratories *Specifications of Cargille Optical Liquids* www.Cargille.com
[14] Crassous J, Gabay C, Liogier G and Berge B 2004 Liquid lens based on electrowetting: a new adaptative component for imaging applications in consumer electronics *Proc. SPIE* **5639** 143